frontiers | Frontiers in Marine Science

TYPE Original Research
PUBLISHED 02 August 2022
DOI 10.3389/fmars.2022.974501

OPEN ACCESS

EDITED BY
Hongyu Ma,
Shantou University, China

REVIEWED BY
Ardavan Farhadi,
Hainan University, China
Biswaranjan Paital,
Orissa University of Agriculture and Technology, India

*CORRESPONDENCE
Huan Wang
wanghuan1@nbu.edu.cn
Chunlin Wang
wangchunlin@nbu.edu.cn

SPECIALTY SECTION
This article was submitted to Aquatic Physiology, a section of the journal Frontiers in Marine Science

RECEIVED 21 June 2022
ACCEPTED 11 July 2022
PUBLISHED 02 August 2022

CITATION
Liang G, Qin K, Chen Y, Niu M, Wang H, Wang C, Mu C, Chen L, Wang F, Su Q and Zhu R (2022) Transcriptomic analysis of adaptive mechanisms in response to inland saline-alkaline water in the mud crab, *Scylla paramamosain*. *Front. Mar. Sci.* 9:974501. doi: 10.3389/fmars.2022.974501

Transcriptomic analysis of adaptive mechanisms in response to inland saline-alkaline water in the mud crab, *Scylla paramamosain*

Guoling Liang[1], Kangxiang Qin[1], Yuhao Chen[1], Mingming Niu[1], Huan Wang[1,2]*, Chunlin Wang[1,2]*, Changkao Mu[1,2], Lizhi Chen[3], Fangfang Wang[3], Qiong Su[4] and Ritong Zhu[5]

[1]School of Marine Science, Ningbo University, Ningbo, China, [2]Key Laboratory of Aquacultural Biotechnology Ministry of Education, Ningbo University, Ningbo, China, [3]Aquatic Technology Promotion Station, Sanmen Rural Bureau, Taizhou, China, [4]Guangxi Engineering Technology Research Center of Breeding of New Mariculture Varieties, Guangxi Institute of Oceanology Co., Ltd., Beihai, China, [5]Aquatic Technology Promotion Station, Yanjin Rural Bureau, Xinxiang, China

Scylla paramamosain is an important marine aquaculture crustacean on the southeastern coast of China. Given the difficulties of overcrowded coastal aquaculture space and insufficient production, inland saline-alkaline water culture has the potential to alleviate this bottleneck. This study separated 600 crabs into four groups: normal salinity (12-18 ppt, NS), coastal low salinity (3-5 ppt, CS), inland low salinity saline-alkaline (1.5 ppt, IS), and acute low salinity (23 ppt down to 3 ppt, AS), followed by a transcriptomic analysis of the gills. CS-vs-NS, IS-vs-NS, and AS-vs-NS obtained 1154, 1012, and 707 DEGs, respectively. GO analysis showed that the DEGs of the three comparison groups were mainly involved in cellular process, metabolic process, biological regulation, organelle, membrane, extracellular region, binding, and catalytic activity. The findings demonstrate that a significant number of genes are engaged in controlling metabolic processes in the osmoregulation process, and that cell membrane catalysis and different enzymes play a vital part in the environmental adaption process. KEGG enrichment analysis revealed that IS possesses a considerable number of signaling pathways that play important roles in osmoregulation when compared to NS. The cAMP signaling pathway increased the expression of CaM and Na^+/K^+-ATPase. These findings show that cations like Ca^{2+}, Na^+, and K^+ are critical for *S. paramamosain* to adapt to inland low salinity saline-alkaline water, and that the cAMP signaling pathway regulates their levels. This research provides a theoretical foundation for improving the saline-alkaline aquaculture technology of *S. paramamosain*.

KEYWORDS

***scylla paramamosain*, inland saline-alkaline water, transcriptomic analysis, low salinity, adaptive mechanisms**

Introduction

Soil salinization is a global problem that affects both developing and developed countries. It affects around 20% of the world's agricultural land and nearly half of the world's irrigated lands (Kumari et al., 2021). Salinization not only affects the productivity of the land and threatens the sustainability of agriculture, but it can also lead to wetland degradation, resulting in imbalances in ecosystems that affect biodiversity (Herbert et al., 2015). This is particularly important where irrigation waters are compromised by salinity as this directly affects food production. Salinity thus intersects with major global concerns, including food security, desertification, and biodiversity protection. (Bal et al., 2021; Harper et al., 2021). Developing strategies to make use of saline land will be crucial for addressing the problem of meeting the challenge of providing food security for the projected global population of 9.3 billion people by 2050 (Liu and Wang, 2021). The advent of aquaculture technology has opened up new options for the conversion of underutilized saline land natural resources into productive resources. The growing demand for aquatic products, however, has pushed aquaculturists to favor inland aquaculture because of the restricted yield of caught fisheries, as well as the expensive cost of coastal land, tight regulations, and environmental concerns. Furthermore, inland ground saline water is unsuitable for traditional agriculture in many regions of the world, piquing aquaculturists' interest in inland saline aquaculture (Li et al., 2017).

There are approximately 99.13 million hectares of saline-alkaline land areas in China, which are primarily situated in the north, northeast, and northwest portions of the country, yet, these limited land resources could be transformed into great potential for fisheries development (Zhang and Wang, 2021). In China's Henan, Shandong, Ningxia, etc., there have been fishery development and utilization of saline-alkaline water resources, which has created a new way for the development and utilization of saline-alkaline water resources (Chen et al., 2020). Inland saline-alkaline waters are rich in resources, but conventional breeding species struggle to survive due to the high salinity, alkalinity, pH values, and complex ionic composition of such waters, severely limiting the development and utilization of saline-alkaline waters. Land-based aquaculture employing inland saline-alkaline groundwater is referred to as inland saline-alkaline waters culture. The ionic composition of inland saline-alkaline waters differs from that of coastal saltwater, and identifying species that are tolerant of these changes is one of the most difficult aspects of the inland saline-alkaline water culture. *Litopenaeus Vannamei* (Roy et al., 2010) and Nile tilapia (Zhao et al., 2015; Zhao et al., 2020) are currently the most popular marine species for inland saline-alkaline water farming.

Mud crab, *Scylla paramamosain* is distributed along the coast of the South China Sea (Chung and Lin, 2006). Because of its abundance, fast growth rate and high market value, the species is an important aquaculture crab in China. mud crab inhabits waters of salinity around 5-33 ppt (Niu et al., 2020). Even though the mud crab adapted to survive in a wide range of salinity, changes in salinity beyond its range of osmoregulation capacity of it can lead to individual death, resulting in severe production losses (Xu et al., 2017). Changes in salinity had a significant effect on the growth and moltin of mud crab (Qi et al., 2013; Ji et al., 2022). Zhang et al. (2020) previously reported transcriptome analysis of *S. paramamosain* under salinity stress. Expression patterns under low and high salinity conditions has been compared with normal salinity to absorb the salinity stress and recognize osmoregulation-related genes of the mud crab, indicated that the mud crab might regulate some mechanisms such as metabolism, immunity responses, and osmoregulation to adapt to the alteration of the low salinity environment. Salinity also affects the nutritional quality of mud crab, it reared at high salinity had better nutritional value than that at low salinity (Wu et al., 2019). The adaptability of mud crab to environmental salinity is mainly reflected in the ability to regulate osmotic pressure and ion concentration. The gills are the most essential organ in the osmoregulation process (Romano and Zeng, 2012). The osmoregulation of the posterior gills allows the mud crab to maintain normal physiological function when the water salinity changes (Wang et al., 2018a; Wang et al., 2018b).

In 2017, our research team began investigating the aquaculture mode of *S. paramamosain* in the saline-alkaline land of the Yellow River basin, and in 2018 they successfully established the inland low salinity saline-alkaline water (1.5-2ppt) aquaculture technology system, with yield per acre reaching the coastal medium level, marking the first time that *S. paramamosain* has been successfully cultured in inland saline-alkaline. However, the molecular mechanism of the adaptation of *S. paramamosain* to inland low-salinity saline-alkaline water has yet to be discovered. Therefore, in the present study, *S. paramamosain* was cultured in normal salinity (12-18ppt), coastal low salinity (3-5ppt), and inland low salinity saline-alkaline water (1.5-2ppt), and acute low salinity (23ppt dropped to 3ppt), respectively. Then, the molecular mechanism of gill responses to inland low salinity saline-alkaline water stress by transcriptomic analysis, to further improve inland saline-alkaline water aquaculture technology.

Materials and methods

Animals and experimental conditions

A total of 600 crabs weighing 30 ± 5g were randomly selected from Sanmen Bay (Zhejiang, China), and each group of 50 crabs (n=3) was transferred to the following 4 experimental ponds

with the same domestication conditions: normal salinity group (NS), coastal low salinity group (CS), inland low salinity saline-alkaline group (IS) and acute low salinity group (AS). NS, located in Sanmen Bay on the eastern coast of Zhejiang, China, is one of the main producing areas of mud crabs, with a salinity of 12-13ppt (as control). CS, located in Hangzhou Bay, northeastern Zhejiang, China, is affected by river inflow and precipitation, the seawater salinity is low and unstable, with a salinity of 3-5ppt. IS, located in Yanjin on the north bank of the Yellow River in Henan, China, the breeding water is saline-alkaline water, and the mud crab is successfully adapted to inland low salinity saline-alkaline water culture after domestication, with a salinity of 1.5-2ppt. AS, located at Ningbo University, Zhejiang, China, normal salinity (12-13ppt) acclimated crabs were directly transferred to diluted 3ppt seawater. Crabs were held in a 30 m^3 cement pond with disinfected seawater and fed once daily in the afternoon (5:00 pm) with razor clam *Sinonovacula constricta* at approximately 10% body weight. The experiment was conducted at ambient temperature and natural photoperiod. Water quality parameters were monitored every morning. The parameters were as followed: water temperature 25-30°C, dissolved oxygen 5.24-7.52 mg L^{-1}, ammonia nitrogen concentration 0.16-1.58 mg L^{-1}, nitrite concentration 0.009-0.102 mg L^{-1}, pH 7.8-8.6, alkalinity 115-160 mg/L $CaCO_3$.

NS, CS and IS crabs were long-term cultured and sampled on day 90, respectively. According to a previous study (Wang et al., 2018a), AS was sampled at 120 h. On each sampling day, crabs were collected from the respective pond with traps and transferred to the laboratory for sampling. the crabs were soaked in iced water until anesthetized and then dissected promptly. The posterior gills of each individual were separated immediately with sterile forceps, frozen in liquid nitrogen, and stored at −80°C for further analysis of transcriptomic. For the collection of the posterior gills, three replicates were set up at the treatment.

RNA extraction and RNA-seq

RNA was extracted from crabs in NS, CS, IS and AS groups, respectively. Total RNA was extracted using the mirVana miRNA Isolation Kit (Ambion) following the manufacturer's protocol. RNA integrity was evaluated using the Agilent 2100 Bioanalyzer (Agilent Technologies, Santa Clara, CA, USA). The samples with RNA Integrity Number (RIN) ≥ 7 were subjected to the subsequent analysis. The libraries were constructed using TruSeq Stranded mRNA LTSample Prep Kit (Illumina, San Diego, CA, USA) according to the manufacturer's instructions. Then these libraries were sequenced on the Illumina sequencing platform (HiSeqTM 2500) and 125bp/150bp paired-end reads were generated.

Analysis of sequencing data

Raw data (raw reads) were processed using Trimmomatic (Bolger et al., 2014). The reads containing ploy-N and the low-quality reads were removed to obtain the clean reads. Then the clean reads were mapped to the reference genome using hisat2 (Kim et al., 2015).

Analysis of differentially expressed transcript (DEGs)

FPKM (Kim et al., 2015) and read counts value of each transcript (protein_coding) was calculated using bowtie2 (Langmead and Salzberg, 2012) and eXpress (Roberts and Pachter, 2013). DEGs were identified using the DESeq (Anders and Huber, 2013) functions estimateSizeFactors and nbinomTest. p value < 0.05 and foldchange >2 or foldchange < 0.5 was set as the threshold for significantly differential expression.

Cluster analysis, GO, and KEGG enrichment

Hierarchical cluster analysis of DEGs was performed to explore transcripts expression patterns. GO enrichment and KEGG (Kanehisa et al., 2008) pathway enrichment analysis of DEGs were respectively performed using R based on the hypergeometric distribution.

Quantitative real-time PCR for RNA-seq results validation

Nine genes were screened out for RNA-seq validation using quantitative real-time PCR (qRT-PCR) with TB Green® Premix Ex Taq™ II (Takara Biomedical Technology Co., Ltd, Beijing, China) according to the manufacturer's instructions.

Results

Sequencing analysis

A total of 12 samples were sequenced in this study, and a total of 80.69 G of clean data was obtained through the Illumina sequencing platform. The effective data volume of each sample is distributed at 6.18-7.02 G, the Q30 base is distributed at 93.0-93.67%, and the average GC content is 48.12% (Table 1). The clean reads were aligned to the reference genome, and the genome alignment of each sample was obtained. Based on the comparison

TABLE 1 Sequencing sample data and quality control.

Sample	RawReads	RawBases	CleanReads	CleanBases	ValidBases	Q30	GC
CS_G1	46.24M	6.94G	45.46M	6.37G	91.87%	93.34%	47.53%
CS_G2	49.05M	7.36G	48.10M	6.70G	91.08%	93.34%	49.79%
CS_G3	49.51M	7.43G	48.67M	6.79G	91.47%	93.39%	48.23%
NS_G1	50.37M	7.56G	49.50M	6.93G	91.65%	93.24%	47.75%
NS_G2	49.62M	7.44G	48.75M	6.82G	91.56%	93.31%	47.67%
NS_G3	47.90M	7.18G	47.09M	6.64G	92.35%	93.25%	46.79%
IS_G1	50.05M	7.51G	49.12M	6.89G	91.72%	93.00%	47.07%
IS_G2	50.87M	7.63G	49.98M	7.02G	91.98%	93.36%	49.52%
IS_G3	44.98M	6.75G	44.22M	6.18G	91.62%	93.22%	47.71%
AS_G1	48.16M	7.22G	47.39M	6.66G	92.16%	93.47%	47.43%
AS_G2	49.59M	7.44G	48.83M	6.82G	91.73%	93.67%	49.00%
AS_G3	50.21M	7.53G	49.40M	6.87G	91.23%	93.64%	48.93%

results, protein-coding gene expression analysis was performed. DEGs were screened according to the expression levels of protein-coding genes in different samples, and there were three differential groups (CS-vs-NS, IS-vs-NS, AS-vs-NS).

DEGs expression analysis

In terms of the degree of aggregation of the samples, the distribution distance between IS and the NS, AS, and CS groups is relatively large, but the NS, AS, and CS samples are more clustered (Figure 1A). When combined with the sample correlation analysis, the gene expression of NS, CS, and AS is similar, but there is a big difference with IS (Figure 1B). To elucidate gene expression patterns at different salinities, the numbers of DEGs were compared among the four treatment groups. Compared with NS, CS, IS, and AS obtained 1154 DEGs (689 up-regulated genes and 465 down-regulated genes), 1012 DEGs (580 up-regulated genes and 432 down-regulated genes), and 707 DEGs (340 up-regulated genes and 367down-regulated genes) (Figure 1C), respectively. Interestingly, 117 common DEGs were found in the three comparison groups (Figure 1D). Of the 117 DEGs, 11 were found without any description, 12 were not annotated in GO and KEGG, 28 were described as "hypothetical", and 6 were described as uncharacterized protein, so these 57 DEGs were excluded. Finally, 60 DEGs with GO annotations were screened and plotted as a heatmap.

The heatmap shows the expression of common DEGs between NS and CS, IS, and AS. Among the 60 common DEGs, 22 were up-regulated and 34 were down-regulated. In addition, cuticle protein AM1159 (CAFS_SP_G_142498.path1) and arthrodial cuticle protein AMP13.4 (CAFS_SP_G_46684.path1) down-regulated in CS-vs-NS and AS-vs-NS, but up-regulated in IS-vs-NS. Y+L amino acid transporter 2 (CAFS_SP_G_140820.path1) up-regulated in CS-vs-NS and IS-vs-NS, but down-regulated in AS-vs-NS. Cytochrome P450 CYP2B (CAFS_SP_G_17938.path1) down-regulated in CS-vs-NS and IS-vs-NS and up-regulated in AS-vs-NS (Figure 2A, Table 2). In IS-vs-NS, serine proteinase stubble (CAFS_SP_G_108715.path1, 4.45-fold) was the most up-regulated, followed by neurotrypsin-like (CAFS_SP_G_30842.path1, 3.74-fold) and crustacean calcium-binding protein 23 (CAFS_SP_G_104586.path1, 3.67-fold) (Figure 2B, Table 2). The expression of these common DEGs indicated that they played an important role in the adaptation of *S. paramamosain* to low salinity.

GO functional annotation

To better understand how different low salinity affects the osmoregulation process of *S. paramamosain*, all DEGs (CS-vs-NS, IS-vs-NS, AS-vs-NS) were subjected to GO analysis to determine their main functions. GO annotations were divided into three types: biological process, cellular component and molecular function.

The main significant processes of DEGs in CS-vs-NS group, IS-vs-NS group and AS-vs-NS group involved involved cellular process, metabolic process, biological regulation, organelle, membrane, extracellular region, binding, and catalytic activity (Figure S1). This indicates that there are many genes involved in regulating metabolic activities in the osmoregulation process, and the catalysis of the cell membrane and various enzymes plays an important role in the process of environmental adaptation.

KEGG enrichment analysis of DEGs

We performed comparative analysis through the KEGG pathway to identify the enrichment pathways for DEGs. Differential genes are classified into six categories according to their functions, including metabolism, genetic information

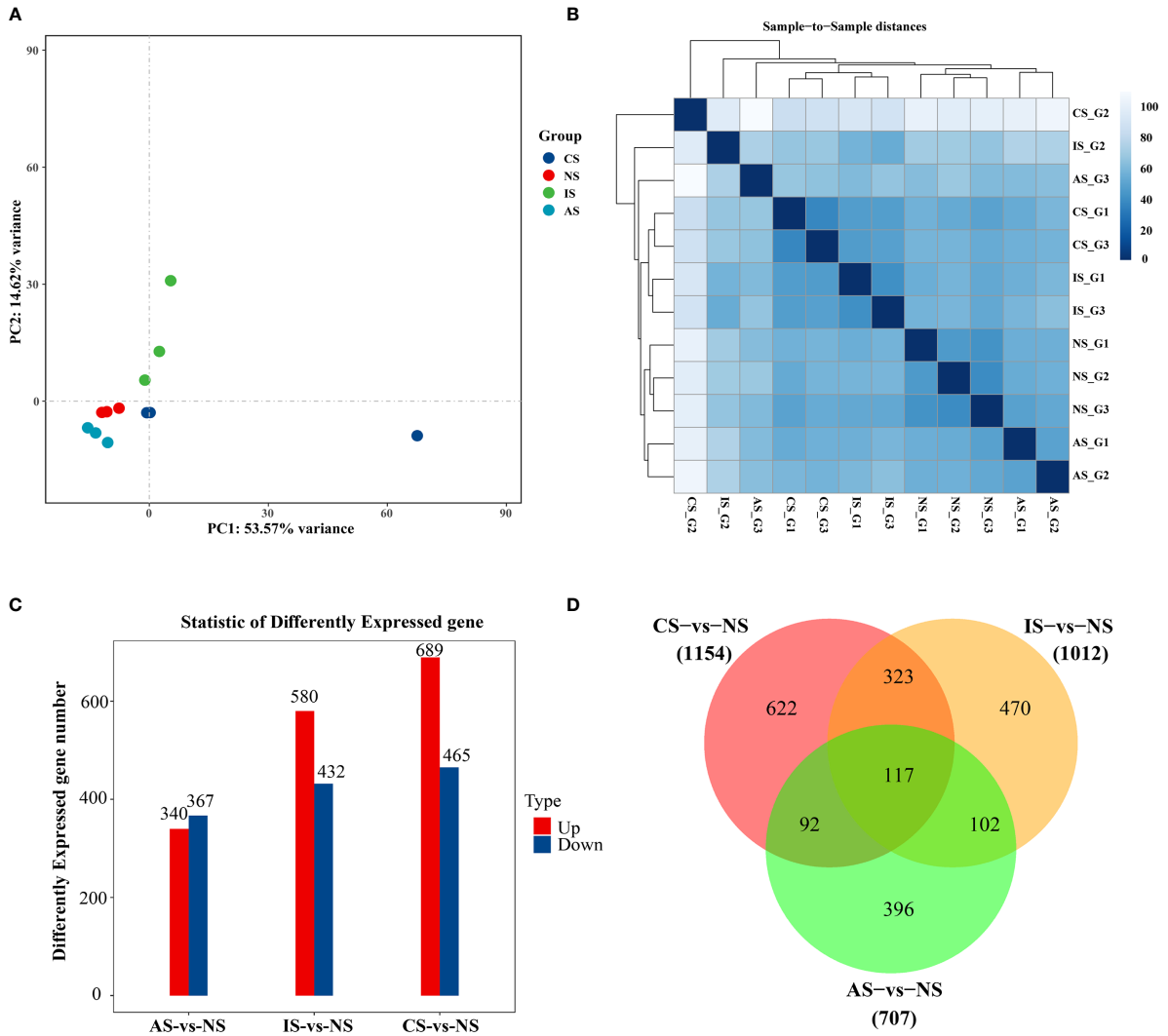

FIGURE 1
Differential gene expression analysis. **(A)** PCA diagram. **(B)** Cluster analysis results. **(C)** Bar Chart. **(D)** VennGraph. In **(A)**, dots represent samples, colors represent groups. In **(B)**, the horizontal axis represents the sample name, the vertical axis represents the corresponding sample name, and the color represents the size of the correlation coefficient. Foldchange> = 2.00 and adjusted p-value <= 0.05.

processing, environmental information processing, cellular processes, organismal systems, and human diseases.

In the CS-vs-NS group, the pathways significantly enriched in the KEGG Enrichment top 20 are mainly related to Energy metabolism, Amino acid metabolism, Carbohydrate metabolism, Carbohydrate metabolism and Lipid metabolism, such as Oxidative phosphorylation, Valine, leucine and isoleucine degradation, propanoate metabolism, citrate cycle (TCA cycle), fatty acid degradation, pyruvate metabolism, glyoxylate and dicarboxylate metabolism, glycine, serine and threonine metabolism, glycolysis/gluconeogenesis, glycerolipid metabolism and fatty acid biosynthesis (Figure 3A). In the IS-vs-NS group, the top 20 pathways showed that eight pathways were directly related to the expression regulation of the Na^+/K^+-ATPase: cardiac muscle contraction, thyroid hormone synthesis, pancreatic secretion, salivary secretion, protein digestion and absorption, proximal tubule bicarbonate reclamation, carbohydrate digestion and absorption, and bile secretion (Figure 3B). In the AS-vs-NS group, the pathways significantly enriched mainly include aminoacyl-tRNA biosynthesis, Nitrogen metabolism, renin-angiotensin system, antifolate resistance, ECM-receptor interaction, ABC transporters, AGE-RAGE signaling pathway in diabetes, alanine, aspartate and glutamate complications metabolism, cytosolic DNA-sensing pathway, and PI3K-Akt signaling pathway, etc. (Figure 3C).

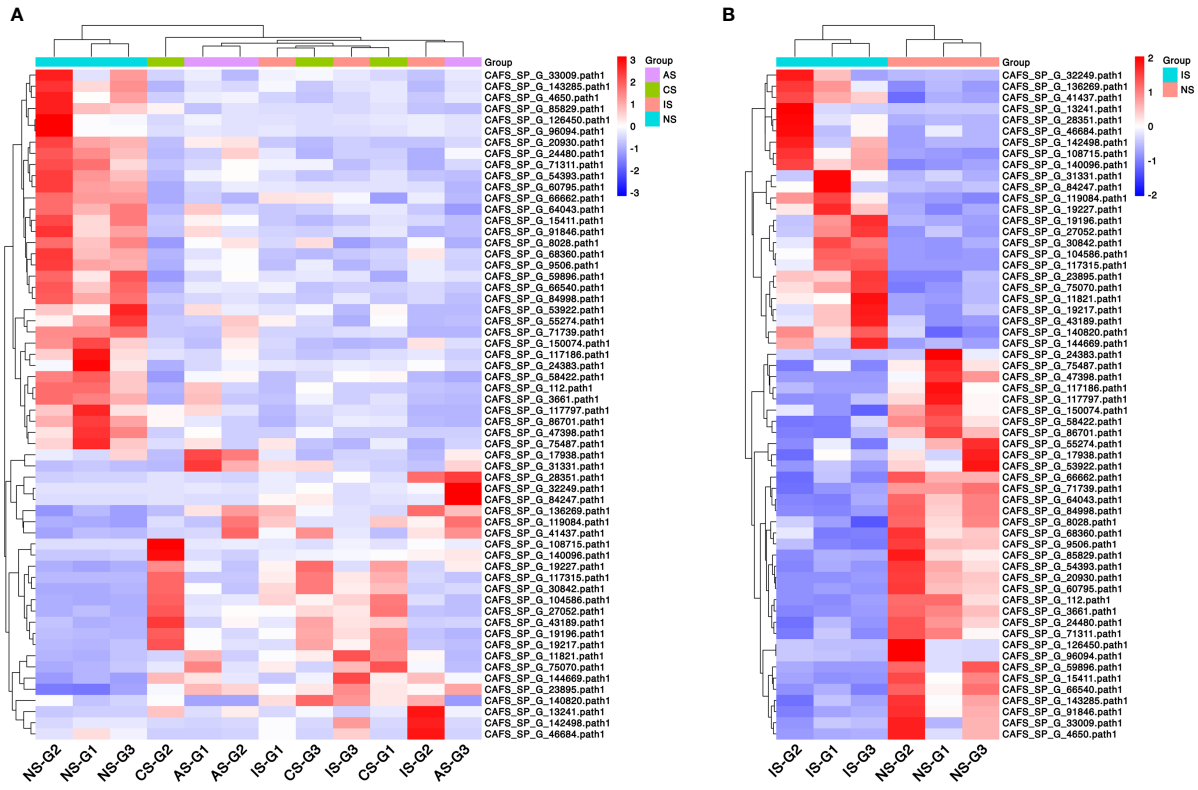

FIGURE 2
Clustered heatmap of common differentially expressed genes (DEGs). **(A)** Common DEGs expression between the three comparison groups. **(B)** DEGs expression of IS-vs-NS. Rows represent DEGs and each column represents one sample. The colors represent the expression level, and red and blue indicate higher and lower expression levels, respectively.

In addition, it was found that the DEGs involved in signal transduction were the most among the three comparison groups (Figure 4). In the IS-vs-NS group, the analysis of the DEGs involved in Signal transduction showed that four significantly signaling pathways were directly related to the expression regulation of the calmodulin (CaM): cGMP-PKG signaling pathway, calcium signaling pathway, cAMP signaling pathway, apelin signaling pathway (Figure S2). Interestingly, the cAMP signaling pathway is also involved in the regulation of Na^+/K^+-ATPase and NMDAR, and its expression levels were significantly up-regulated by 2.115-fold and 6.064-fold, respectively (Figure 5).

Validity of DEGs in transcriptomic data

To validate the RNA sequencing, nine genes were selected and quantified using qPCR, namely Uricase-like (UL), TNFSF, partial (TNFSF), Homeotic protein empty spiracles-like (HPES), Amino acid/polyamine transporter I (AATI), Cytochrome P450 CYP2B(CP450), Aminopeptidase N-like (ANL), Estrogen sulfotransferase (ES), WD repeat-containing protein 47 (WDRCP), Laminin subunit gamma-1-like isoform X1 (LSGIX). The relative expression tendencies of the nine genes were in accordance with the RNA-seq (Figure 6), validating the results of the mRNA sequencing analysis.

Discussion

S. paramamosain is an important marine aquaculture crustacean (Tang et al., 2020). In 2017, our research team began investigating the aquaculture mode of *S. paramamosain* in the saline-alkaline water of the Yellow River basin, and in 2018 we successfully established the inland low salinity saline-alkaline water (1.5-2ppt) breeding technology system, with yield per acre reaching the coastal medium level, marking the first time that *S. paramamosain* has been successfully cultured in inland saline-alkaline. However, the molecular mechanism by which *S. paramamosain* responds to saline-alkaline water stress with reduced salinity has yet to be discovered. As a result, we investigated the transcriptomic analysis of *S. paramamosain* gills cultivated in normal salinity, coastal low salinity, inland low salinity saline-alkaline water, and acute low salinity, respectively.

TABLE 2 Differentially expressed genes annotation.

Gene ID	Description	log2FoldChange (CS-vs-NS)	log2FoldChange (IS-vs-NS)	log2FoldChange (AS-vs-NS)
CAFS_SP_G_108715.path1	Serine proteinase stubble [*Portunus trituberculatus*]	7.18	4.45	3.57
CAFS_SP_G_30842.path1	Neurotrypsin-like [*Penaeus vannamei*]	5.17	3.74	2.88
CAFS_SP_G_117315.path1	Putative family 31 glucosidase KIAA1161 [*Portunus trituberculatus*]	5.13	3.53	1.40
CAFS_SP_G_104586.path1	Crustacean calcium-binding protein 23 [*Portunus trituberculatus*]	4.73	3.67	2.49
CAFS_SP_G_19217.path1	Aminopeptidase N-like [*Penaeus vannamei*]	4.46	2.32	2.01
CAFS_SP_G_19196.path1	Aminopeptidase N [*Portunus trituberculatus*]	4.34	2.62	1.80
CAFS_SP_G_84247.path1	Ubiquitin carboxyl-terminal hydrolase 7 isoform X5 [*Trichoplusia ni*]	4.00	3.62	5.75
CAFS_SP_G_43189.path1	AN1-type zinc finger protein 4 [*Portunus trituberculatus*]	3.71	1.97	1.63
CAFS_SP_G_19227.path1	Aminopeptidase N-like [*Penaeus vannamei*]	3.45	1.80	1.75
CAFS_SP_G_27052.path1	Sarcosine dehydrogenase, mitochondrial [*Portunus trituberculatus*]	3.15	1.63	1.29
CAFS_SP_G_140096.path1	Branched-chain-amino-acid aminotransferase, cytosolic-like [*Penaeus vannamei*]	3.06	1.61	1.09
CAFS_SP_G_32249.path1	Ubiquitin carboxyl-terminal hydrolase 7 isoform X2 [*Diachasma alloeum*]	2.64	2.25	5.06
CAFS_SP_G_41437.path1	Friend leukemia integration 1 transcription factor [*Portunus trituberculatus*]	2.37	2.20	2.90
CAFS_SP_G_144669.path1	DNA repair protein RAD51 4 [*Portunus trituberculatus*]	2.35	2.47	1.72
CAFS_SP_G_13241.path1	Phospholipase A2 isozymes PA3A/PA3B/PA5 [*Portunus trituberculatus*]	2.27	2.60	1.44
CAFS_SP_G_75070.path1	Putative urea transporter 1-like [*Penaeus vannamei*]	2.16	1.93	1.62
CAFS_SP_G_11821.path1	Sulfotransferase 1 family member D1-like [*Penaeus vannamei*]	2.00	2.16	1.20
CAFS_SP_G_31331.path1	Angiopoietin-4 [*Portunus trituberculatus*]	1.77	1.74	3.34
CAFS_SP_G_23895.path1	LOW QUALITY PROTEIN: probable tRNA N6-adenosine Threonylcarbamoyltransferase, Mitochondrial [*Penaeus vannamei*]	1.55	1.53	1.53
CAFS_SP_G_136269.path1	Estrogen sulfotransferase [*Portunus trituberculatus*]	1.35	2.15	2.02
CAFS_SP_G_28351.path1	Fatty acid synthase, partial [*Portunus trituberculatus*]	1.25	3.08	2.72
CAFS_SP_G_119084.path1	Translation initiation factor IF-2, mitochondrial-like [*Penaeus vannamei*]	1.14	1.10	1.35
CAFS_SP_G_140820.path1	PREDICTED: Y+L amino acid transporter 2 [*Dinoponera quadriceps*]	1.13	1.08	-1.47
CAFS_SP_G_8028.path1	Netrin-1 [*Portunus trituberculatus*]	-1.02	-1.19	-1.02
CAFS_SP_G_15411.path1	laminin subunit gamma-1-like isoform X1 [*Penaeus vannamei*]	-1.08	-1.26	-1.06
CAFS_SP_G_55274.path1	Peptidase S9 prolyl oligopeptidase catalytic domain [*Trinorchestia longiramus*]	-1.12	-1.58	-1.23
CAFS_SP_G_9506.path1	Zinc finger protein [*Armadillidium vulgare*]	-1.14	-1.37	-1.14
CAFS_SP_G_71311.path1	Colorectal mutant cancer protein [*Portunus trituberculatus*]	-1.17	-1.61	-1.34
CAFS_SP_G_86701.path1	Multiple epidermal growth factor-like domains protein 6 [*Portunus trituberculatus*]	-1.19	-2.24	-2.19
CAFS_SP_G_53922.path1	IDLSRF-like peptide [*Cephus cinctus*]	-1.21	-2.20	-1.36
CAFS_SP_G_117797.path1	Multiple epidermal growth factor-like domains protein 6 [*Portunus trituberculatus*]	-1.25	-2.62	-1.59
CAFS_SP_G_58422.path1	Putative metalloprotease TIKI1-like [*Penaeus vannamei*]	-1.25	-1.40	-1.32
CAFS_SP_G_60795.path1	Protein sprint [*Portunus trituberculatus*]	-1.30	-1.23	-1.54
CAFS_SP_G_75487.path1	PREDICTED: NACHT and WD repeat domain-containing Protein 2-like [*Hyalella azteca*]	-1.31	-1.69	-1.38
CAFS_SP_G_24383.path1	Amino acid/polyamine transporter I [*Trinorchestia longiramus*]	-1.38	-1.02	-1.43
CAFS_SP_G_33009.path1	Cubilin [*Penaeus vannamei*]	-1.49	-1.68	-1.94
CAFS_SP_G_64043.path1	Gamma-butyrobetaine dioxygenase-like isoform X2 [*Penaeus vannamei*]	-1.50	-1.62	-1.45

(Continued)

TABLE 2 Continued

Gene ID	Description	log2FoldChange (CS-vs-NS)	log2FoldChange (IS-vs-NS)	log2FoldChange (AS-vs-NS)
CAFS_SP_G_85829.path1	Aquaporin-3-like [*Penaeus vannamei*]	-1.55	-2.91	-3.35
CAFS_SP_G_24480.path1	WD repeat-containing protein 47, partial [*Penaeus vannamei*]	-1.62	-1.57	-1.06
CAFS_SP_G_4650.path1	MD2 domain protein general type [*Hemigrapsus sanguineus*]	-1.71	-1.95	-1.47
CAFS_SP_G_112.path1	Glycogen-binding subunit 76A [*Portunus trituberculatus*]	-1.74	-2.39	-1.50
CAFS_SP_G_3661.path1	DNA-directed RNA polymerase III subunit RPC4 [*Portunus trituberculatus*]	-1.78	-2.50	-1.59
CAFS_SP_G_91846.path1	Leucine–tRNA ligase, cytoplasmic [*Portunus trituberculatus*]	-1.80	-2.12	-1.51
CAFS_SP_G_66662.path1	Tyrosine-protein kinase RYK-like [*Penaeus vannamei*]	-1.90	-1.09	-2.50
CAFS_SP_G_17938.path1	Cytochrome P450 CYP2B [*Eriocheir sinensis*]	-1.92	-1.29	1.24
CAFS_SP_G_54393.path1	Protein kinase DC2 [*Portunus trituberculatus*]	-1.96	-1.96	-1.62
CAFS_SP_G_150074.path1	Serine protease inhibitor dipetalogastin [*Portunus trituberculatus*]	-1.98	-1.53	-1.62
CAFS_SP_G_71739.path1	Potassium voltage-gated channel subfamily H member 1 ether-a-go-go, partial [*Homarus americanus*]	-2.00	-2.45	-1.93
CAFS_SP_G_143285.path1	TNFSF, partial [*Procambarus clarkii*]	-2.03	-1.82	-1.85
CAFS_SP_G_66540.path1	Uricase-like [*Penaeus vannamei*]	-2.35	-1.81	-1.86
CAFS_SP_G_59896.path1	Glutamine synthetase [*Portunus trituberculatus*]	-2.46	-1.41	-1.49
CAFS_SP_G_46684.path1	Arthrodial cuticle protein AMP13.4 [*Callinectes sapidus*]	-2.69	1.62	-2.84
CAFS_SP_G_20930.path1	Protein turtle-like [*Penaeus vannamei*]	-2.75	-2.51	-1.26
CAFS_SP_G_142498.path1	Cuticle protein AM1159 [*Portunus trituberculatus*]	-2.76	3.49	-3.59
CAFS_SP_G_117186.path1	Multiple epidermal growth factor-like domains protein 6 [*Portunus trituberculatus]*	-2.99	-2.95	-2.49
CAFS_SP_G_47398.path1	Neuropeptide F receptor [*Portunus trituberculatus*]	-3.35	-5.31	-3.48
CAFS_SP_G_68360.path1	Nicotinamide phosphoribosyltransferase-like [*Penaeus vannamei*]	-3.54	-2.05	-2.01
CAFS_SP_G_84998.path1	Homeotic protein empty spiracles-like [*Penaeus vannamei*]	-4.07	-2.82	-3.56
CAFS_SP_G_126450.path1	Zinc transporter ZIP1 [*Portunus trituberculatus*]	-4.52	-3.36	-3.30
CAFS_SP_G_96094.path1	Zinc transporter ZIP1 [*Portunus trituberculatus*]	-4.78	-3.43	-3.76

To analyze the molecular mechanism of *S. paramamosain* responds to inland low salinity saline-alkaline water stress at the transcriptional level, and to provide theoretical reference for improving inland saline-alkaline water aquaculture technology.

Under low salinity seawater stress, *S. paramamosain* can acquire adaptive capacity through osmoregulation and reach an adaptive state after 120 h (Wang et al., 2018a). The osmoregulation of *S. paramamosain* is to compensate and

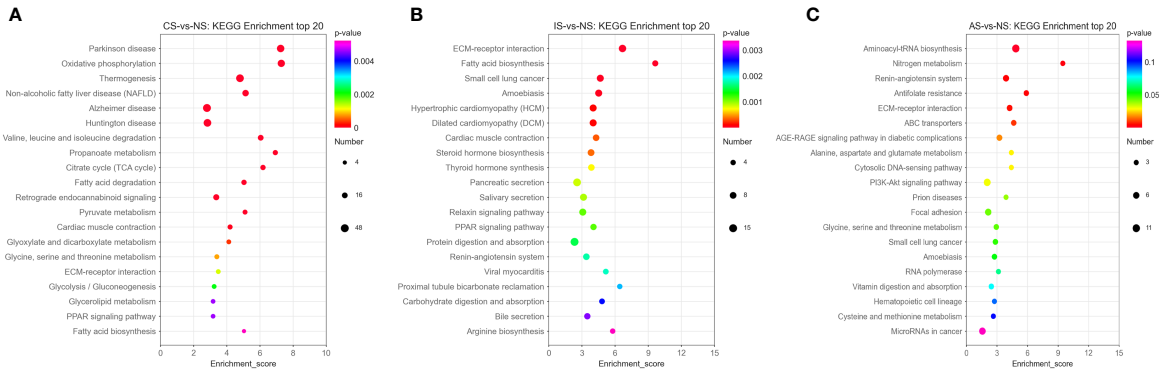

FIGURE 3
Pathway functional enrichment of differentially expressed genes (DEGs). **(A)** CS-vs-NS group. **(B)** IS-vs-NS group. **(C)** AS-vs-NS group. X axis represents enrichment score. Y axis represents pathway name. The color indicates the q value, the lower p-value indicates the more significant enrichment. Point size indicates DEG number (The larger dots refer to a larger amount).

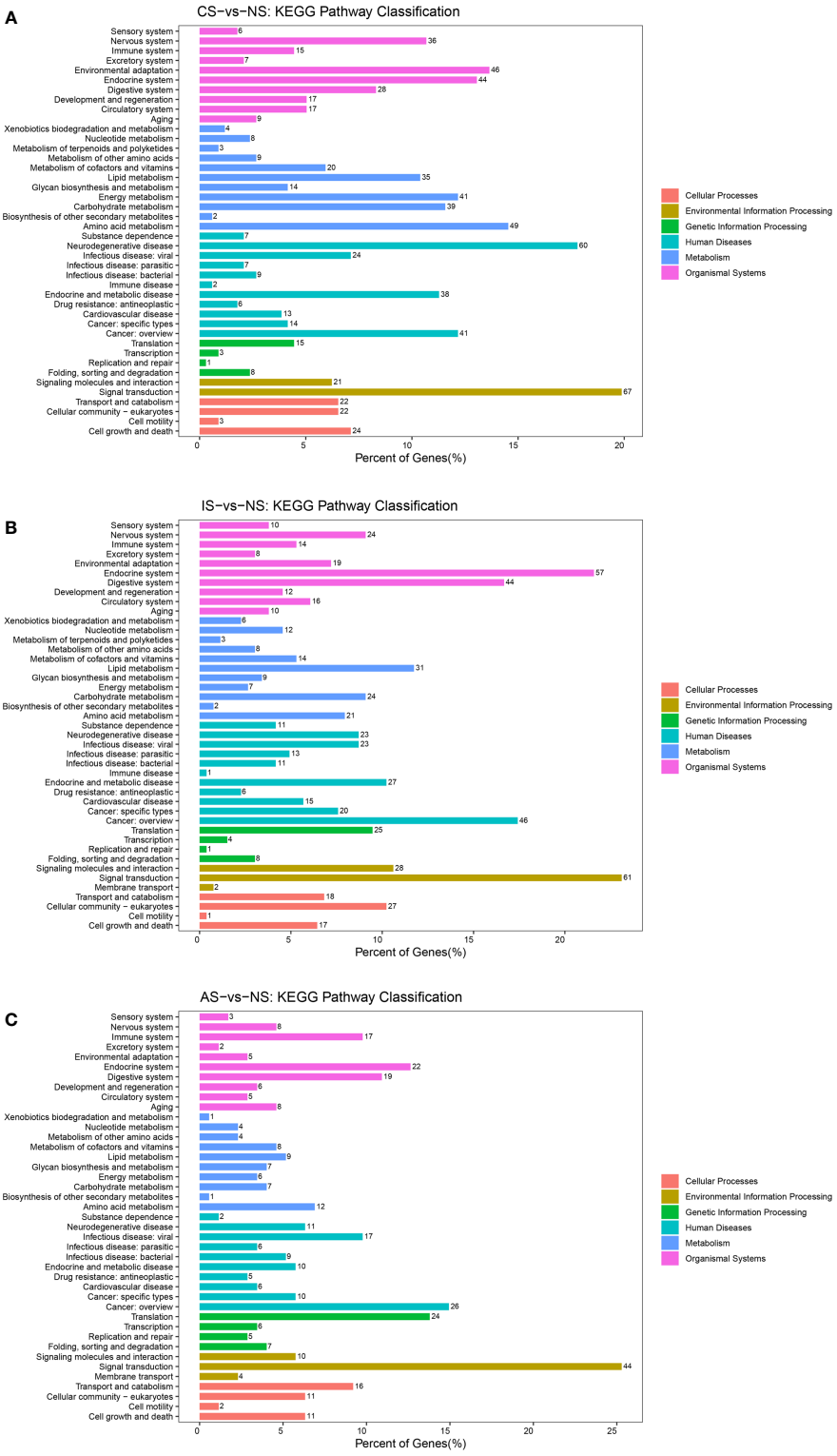

FIGURE 4
KEGG pathways classification. **(A)** CS-vs-NS group. **(B)** IS-vs-NS group. **(C)** AS-vs-NS group. There were six branches for KEGG pathways: Cellular Processes, Environmental Information Processing, Genetic Information Processing, Human Disease (For animals only), Metabolism and Organismal Systems.

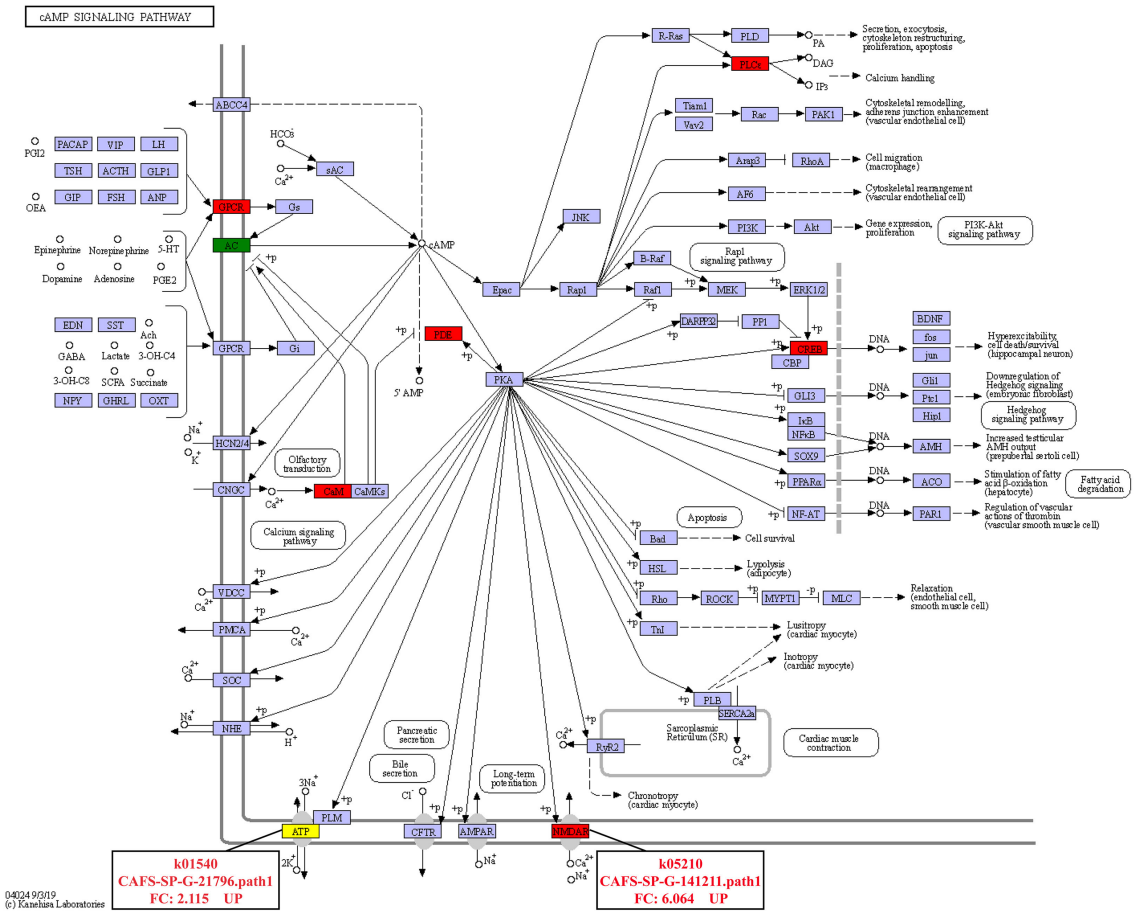

FIGURE 5
Pathway analysis of cAMP signaling pathway (ko04024) in IS-vs-NS.

transport ions through the posterior gills to regulate hemolymph ion concentration (Yao et al., 2020), which determines hemolymph osmotic pressure (Lignot et al., 2000), so the ionic composition and concentration of the water environment will affect its osmoregulation capacity. However, the ionic composition of saline-alkaline water differs greatly from that of seawater, and the posterior gill response mechanism may differ. The results of PCA analysis revealed that there were clear distribution differences between the IS group and the NS, AS, and CS groups, but the NS, AS, and CS groups with the same seawater background but different salinity were more clustered. When combined with the sample correlation analysis, the gene expression of NS, CS, and AS is similar, but there is a significant difference when compared to IS. The high degree of sample dispersion may be due to the differences in the osmoregulation capacity of *S. paramamosain* individuals under the degree of salinity stress. This indicates that the molecular mechanism of *S. paramamosain* adapting to saline-alkaline water may be different from the osmoregulation mechanism of adapting to low salinity seawater stress, but the osmoregulation mechanism of seawater with different salinity has a certain similarity.

Osmoregulation in crustaceans is an energy-consuming process (Yao et al., 2020). Free amino acids are used as energy substrates for physiological stress compensation (Zhou et al., 2011). L-serine levels in the hemolymph and muscle of *Litopenaeus vannamei* increased dramatically with decreasing salinity in earlier research, and osmoregulation by consuming L-serine as an energy source was demonstrated (Shinji et al., 2012). Serine is one of the major amino acids in Serine proteinase's catalytic active site (Shi et al., 2008). We discovered that in a low salinity environment, the expression of serine proteinase stubble was dramatically elevated. CS group was the most up-regulated (7.18-fold) compared to NS group, followed by IS group (4.45-fold) and AS group (3.45-fold) (3.57-fold). This finding may indicate serine proteinase stubble of the gills is the energy source for osmoregulation of *S. paramamosain*.

In crustaceans, gill tissue has been found to modulate ion transport, acclimatization to various salinities, and significant

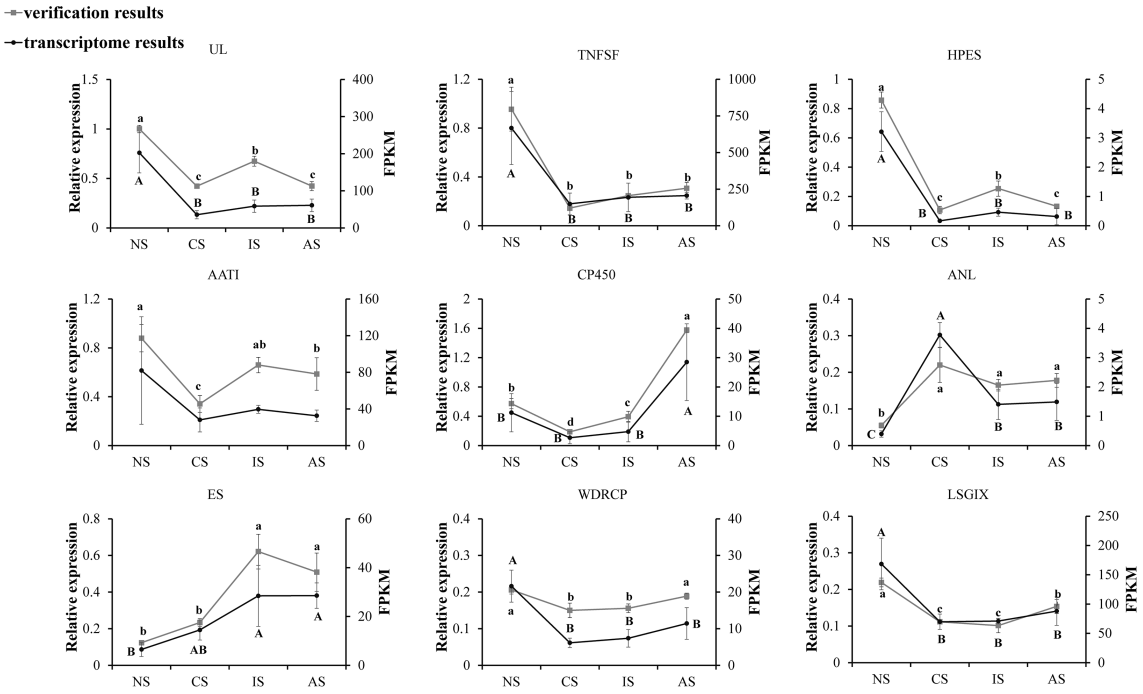

FIGURE 6
Candidate gene expression levels revealed by qRT-PCR and RNA-seq. NS represents normal salinity of 12-13ppt, CS represents coastal low salinity of 3-5ppt, IS represents inland low salinity saline-alkaline water of 1.5-2ppt, AS represents acute low salinity, 3ppt from normal salinity (12-13ppt) directly, which dropped. The different letters above the line chart indicate significant differences.

active areas for osmoregulation (Nikapitiya et al., 2015). Gill filament is the most fundamental functional unit of a gill, and its basic structure is made up of cuticle, subcuticular space, and gill epithelial cells, with cuticle being the most important for osmoregulation (Barra et al., 1983). The major component of the cuticle, cuticle protein, interacts with chitin to maintain the cuticle's structural integrity (Andersen, 1999). Cuticle protein is extremely permeable to the ions Na^+ and Cl^-. The major ions that make up hemolymph's osmotic pressure are Na^+ and Cl^-, which together determine the osmotic pressure of hemolymph (Lignot et al., 2000).

Cuticle protein AM1159 and cuticle protein AMP13.4 were down-regulated by 2.69-fold and 2.76-fold in CS group, down-regulated by 2.84-fold and 3.59-fold in AS group, but up-regulated by 3.49-fold and 1.62-fold in IS group, respectively, compared to NS group. The findings imply that cuticle protein is significant in the adaptation of *S. paramamosain* to inland low salinity saline-alkaline water, but its molecular mechanism needs to be investigated further.

Calcium signaling is important for cell growth, death, and metabolism (Wang et al., 2015; Dubois et al., 2016). Calmodulin (CaM) modulates cellular processes such as stress response, apoptosis, and calcium homeostasis by rapidly increasing the concentration of Ca^{2+} on the cell membrane when cells are stimulated (Tadross et al., 2008; Berchtold and Villalobo, 2014; Wang et al., 2015; Huang et al., 2020). Additionally, Ca^{2+} signal transduction may be a key signaling route for gills to cope with osmotic stress (Marshall et al., 2000; Fiol et al., 2006). CaM is involved in the regulation of Na^+ and Cl^- transport in the posterior gills of *Eriocheir sinensis*, resulting in osmoregulation, according to Péqueux and Gilles (1992). Na^+ and Cl^- transport is the most important osmoregulation method in crustaceans, which is driven by the Na^+/K^+-ATPase (Huang et al., 2020). The Na^+/K^+-ATPase is a membrane protein that connects the exchange of two external K^+ for three internal Na^+ linked to the hydrolysis of a single ATP molecule (Post et al., 1972). Jia and Liu (2018) found that the activity of the Na^+/K^+-ATPase can be controlled by cAMP. Injecting cAMP into *Leptograpsus variegatus* causes the gill filament Na^+/K^+-ATPase to activate quickly (Lucu et al., 2000). IS up-regulated CaM expression in comparison to NS *via* numerous signaling pathways, including the cGMP-PKG signaling system, calcium signaling pathway, cAMP signaling pathway, and apelin signaling pathway. In the cAMP signaling pathway, the expressions of Na^+/K^+-ATPase and NMDAR were dramatically up-regulated. It is no surprise that the osmoregulation related genes including Na^+/K^+-ATPase and NMDAR were upregulated under the low salinity condition. Under salinity stress, the genes related to ion transport will play a very important role in *S. paramamosain*. Zhang et al. (2020)

analyzed transcriptomic changes in ambient salinity challenges of different salinities, indicated that under low salinity stress, *S. paramamosain* might cause induce changes in genes related to ion transport, such as the significant up regulation of Na^+/K^+-ATPase. NMDAR ion channels are highly permeable to Ca^{2+}, Na^+ and K^+ ions (Hansen et al., 2018). Based on the above findings, it is hypothesized that the process of adapting to inland low salinity saline-alkaline water in *S. paramamosain* regulates the expression changes of Na^+/K^+-ATPase and NMDAR *via* the cAMP signaling pathway, improving the transport efficiency of Ca^{2+}, Na^+, and K^+, and finally achieving osmotic pressure balance inside and outside the cell membrane, but the molecular mechanism needs to be investigated further. At the same time, this study also shows that cations such as Ca^{2+}, Na^+, and K^+ are extremely important for *S. paramamosain* to adapt to inland low salinity saline water.

Conclusion

In conclusion, we analyzed the differences in gene expression between normal salinity, coastal low salinity, inland saline-alkaline low salinity, and acute low salinity in the gills of *S. paramamosain*. CS-vs-NS, IS-vs-NS, and AS-vs-NS obtained 1154 (689 up-regulated genes and 465 down-regulated genes), 1012 (580 up-regulated genes and 432 down-regulated genes), and 707 (340 up-regulated genes and 367 down-regulated genes) DEGs, respectively. KEGG enrichment analysis showed that IS has numerous signaling pathways involved in the regulation of CaM and Na^+/K^+-ATPase when compared to NS. The results suggest that the adaptation of *S. paramamosain* to inland low salinity saline-alkaline water regulates the expression changes of Na^+/K^+-ATPase and NMDAR *via* the cAMP signaling pathway, improving Ca^{2+}, Na^+, and K^+ transport efficiency and achieving osmotic pressure balance inside and outside the cell membrane, but the molecular mechanism needs to be investigated further. At the same time, our research reveals that cations like Ca^{2+}, Na^+, and K^+ are critical for *S. paramamosain* to adapt to inland low salinity saline-alkaline water. In this study, the molecular mechanism of *S. paramamosain* adapting to inland low salinity saline-alkaline water was investigated for the first time, and numerous potential genes and KEGG pathways involved in regulation were revealed, to provide a scientific basis for guiding the aquaculture technology of crustaceans aquaculture.

Data availability statement

The data presented in the study are deposited in the National Center for Biotechnology Information (NCBI) Sequence Read Archive (SRA) repository, accession number PRJNA851163.

Author contributions

HW conceived and designed the study. GL performed the cultivation of experimental animals. GL, KQ, YC, MN, CW, CM, LC, FW, QS, and RZ performed and analyzed all other experiments. GL and HW wrote the manuscript with support from all authors. All authors read and approved the final manuscript.

Funding

This study was sponsored by the National Key R&D Program of China (2020YFD0900203), the Sanmen County Agricultural and Rural Bureau, Zhejiang Province (2020-GK088-1), Key Scientific and Technological Grant of Zhejiang for Breeding New Agricultural Varieties (2021C02069-6), Zhejiang Agricultural Science and Technology Cooperation Project (2021SNLF029).

Conflict of interest

Author QS is employed by Guangxi Institute of Oceanology Co., Ltd.

The remaining authors declare that the research was conducted in the absence of any commercial or financial relationships that could be construed as a potential conflict of interest.

Publisher's note

Supplementary material

The Supplementary Material for this article can be found online at: https://www.frontiersin.org/articles/10.3389/fmars.2022.974501/full#supplementary-material

SUPPLEMENTARY FIGURE 1
GO annotation of differentially expressed genes (DEGs). **(A)** CS-vs-NS group. **(B)** IS-vs-NS group. **(C)** AS-vs-NS group. DEGs were assigned to second-tier GO categories associated with three parent terms: biological process, cellular component, and molecular function.

SUPPLEMENTARY FIGURE 2
The signaling pathway involved in regulating CaM in IS-vs-NS. **(A)** Calcium signaling pathway, ko04020. **(B)** cGMP-PKG signaling pathway, ko04022. **(C)** Apelin signaling pathway, ko04371.

References

Andersen, S. O. (1999). Exoskeletal proteins from the crab, cancer pagurus. *Comp. Biochem. Physiol. A Mol. Integr. Physiol.* 123 (2), 203–211. doi: 10.1016/S1095-6433(99)00051-3

Anders, S., and Huber, W. (2013). *Differential expression of RNA-seq data at the gene level – the DESeq package* Vol. 1843 (EMBL), 398–435.

Bal, A., Panda, F., Pati, S. G., Das, K., Agrawal, P. K., and Paital, B. (2021). Modulation of physiological oxidative stress and antioxidant status by abiotic factors especially salinity in aquatic organisms. *Comp. Biochem. Physiol. C Toxicol. Pharmacol.* 241, 108971. doi: 10.1016/j.cbpc.2020.108971

Barra, J. A., Pequeux, A., and Humbert, W. (1983). A morphological study on gills of a crab acclimated to fresh water. *Tissue Cell.* 15 (4), 583–596. doi: 10.1016/0040-8166(83)90009-5

Berchtold, M. W., and Villalobo, A. (2014). The many faces of calmodulin in cell proliferation, programmed cell death, autophagy, and cancer. *Biochim. Biophys. Acta* 1843 (2), 398–435. doi: 10.1016/j.bbamcr.2013.10.021

Bolger, A. M., Lohse, M., and Usadel, B. (2014). Trimmomatic: a flexible trimmer for illumina sequence data. *Bioinformatics* 30 (15), 2114–2120. doi: 10.1093/bioinformatics/btu170

Chen, X. Z., Lai, Q., Mo, Z. L., Gao, H. Y., and Han, Z. X. (2020). Saline alkali water green breeding technology mode. *China Fish.* 9, 61–63.

Chung, K. F., and Lin, H. C. (2006). Osmoregulation and Na,K-ATPase expression in osmoregulatory organs of Scylla paramamosain. *Comp. Biochem. Physiol. A Mol. Integr. Physiol.* 144 (1), 48–57. doi: 10.1016/j.cbpa.2006.02.003

Dubois, C., Prevarskaya, N., and Vanden Abeele, F. (2016). The calcium-signaling toolkit: Updates needed. *Biochim. Biophys. Acta* 1863 (6 Pt B), 1337–1343. doi: 10.1016/j.bbamcr.2015.11.033

Fiol, D. F., Chan, S. Y., and Kültz, D. (2006). Identification and pathway analysis of immediate hyperosmotic stress responsive molecular mechanisms in tilapia (*Oreochromis mossambicus*) gill. *Comp. Biochem. Physiol. Part D Genomics Proteomics* 1 (3), 344–356. doi: 10.1016/j.cbd.2006.08.002

Hansen, K. B., Yi, F., Perszyk, R. E., Furukawa, H., Wollmuth, L. P., Gibb, A. J., et al (2018). Structure, function, and allosteric modulation of NMDA receptors. *J. Gen. Physiol.* 150 (8), 1081–1105. doi: 10.1085/jgp.201812032

Harper, R. J., Dell, B., Ruprecht, J. K., Sochacki, S. J., and Smettem, K. R. J. (2021). Salinity and the reclamation of salinized lands. *Soils Landscape Restor.* 7, 193–208. doi: 10.1016/B978-0-12-813193-0.00007-2

Herbert, E. R., Boon, P., Burgin, A. J., Neubauer, S. C., Franklin, R. B., Ardón, M., et al (2015). A global perspective on wetland salinization: ecological consequences of a growing threat to freshwater wetlands. *Ecosphere* 6, 10, 1–43. Wiley-Blackwell. doi: 10.1890/ES14-00534.1

Huang, S. J., Jiang, S., and Xu, Q. H. (2020). Acute salinity stress in gill Na^+/K^+-ATPase in the swimming crab, *Portunus trituberculatus* (Brachyura, portunidae). *Crustaceana* 93 (6), 587–609. doi: 10.1163/15685403-bja10012

Jia, Y., and Liu, X. (2018). Expression of Na^+/K^+-ATPase was affected by salinity change in pacific abalone haliotis discus hannai. *Front. Physiol.* 9, 1244. doi: 10.3389/fphys.2018.01244

Ji, Z. L., Li, R. H., Wang, C. L., Zhang, Z. Y., Zhang, W. J., Mu, C. K., et al (2022). Effect of long-term low-salinity culture on the survival, growth, and nutrient composition of mud crab Scylla paramamosain. *J. Ocean Univ. China Vol.* 21, 179–185. doi: 10.1007/s11802-022-4812-x

Kanehisa, M., Araki, M., Goto, S., Hattori, M., Hirakawa, M., Itoh, M., et al. (2008). KEGG for linking genomes to life and the environment. *Nucleic Acids Res.* 36, 480–484. doi: 10.1093/nar/gkm882D480-4

Kim, D., Langmead, B., and Salzberg, S. L. (2015). HISAT: a fast spliced aligner with low memory requirements. *Nat. Methods* 12 (4), 357–360. doi: 10.1038/nmeth.3317

Kumari, S., Harikrishna, V., Surasani, V., Balange, A. K., and Rani, B. (2021). Growth, biochemical indices and carcass quality of red tilapia reared in zero water discharge based biofloc system in various salinities using inland saline ground water. *Aquaculture* 540 (9), 736730. doi: 10.1016/j.aquaculture.2021.736730

Langmead, B., and Salzberg, S. L. (2012). Fast gapped-read alignment with bowtie 2. *Nat. Methods* 9 (4), 357–359. doi: 10.1038/nmeth.1923

Lignot, J. H., Spanings-Pierrot, C., and Charmantier, G. (2000). Osmoregulatory capacity as a tool in monitoring the physiological condition and the effect of stress in crustaceans - ScienceDirect. *Aquaculture* 191 (1–3), 209–245. doi: 10.1016/S0044-8486(00)00429-4

Liu, L., and Wang, B. (2021). Protection of halophytes and their uses for cultivation of saline-alkali soil in China. *Biology (Basel)* 10 (5), 353. doi: 10.3390/biology10050353

Li, E., Wang, X. D., Chen, K., Xu, C., Qin, J. G., and Chen, L. Q. (2017). Physiological change and nutritional requirement of pacific white shrimp *Litopenaeus vannamei* at low salinity. *Rev. Aquac.* 9, 57–75. doi: 10.1111/raq.12104

Lucu, C., Devescovi, M., Skaramuca, B., and Kozul, V. V. (2000). Gill Na, K-ATPase in the spiny lobster *Palinurus elephas* and other marine osmoconformers: Adaptiveness of enzymes from osmoconformity to hyperregulation. *J. Exp. Mar. Biol. Ecol.* 246 (2), 163–178. doi: 10.1016/S0022-0981(99)00179-3

Marshall, W. S., Bryson, S. E., and Luby, T. (2000). Control of epithelial cl(-) secretion by basolateral osmolality in the euryhaline teleost fundulus heteroclitus. *J. Exp. Biol.* 203 (Pt 12), 1897–1905. doi: 10.1242/jeb.203.12.1897

Nikapitiya, C., Kim, W. S., Park, K., Kim, J., Lee, M. O., and Kwak, I. S. (2015). Chitinase gene responses and tissue sensitivity in an intertidal mud crab (*Macrophthalmus japonicus*) following low or high salinity stress. *Cell Stress Chaperones* 20 (3), 517–526. doi: 10.1007/s12192-015-0576-1

Niu, J., Hu, X. L., Ip, J. C. H., Ma, K. Y., and Chu, K. H. (2020). Multi-omic approach provides insights into osmoregulation and osmoconformation of the crab Scylla paramamosain. *Sci. Rep.* 10 (1), 21771. doi: 10.1038/s41598-020-78351-w

Péqueux, A., and Gilles, R. (1992). Calmodulin as a modulator of NaCl transport in the posterior salt-transporting gills of the Chinese crab eriocheir sinensis. *Mar. Biol.* 113 (1), 65–69. doi: 10.1007/BF00367639

Post, R. L., Hegyvary, C., and Kume, S. (1972). Activation by adenosine triphosphate in the phosphorylation kinetics of sodium and potassium ion transport adenosine triphosphatase. *J. Biol. Chem.* 247 (20), 6530–6540. doi: 10.1016/S0021-9258(19)44725-X

Qi, L., Gu, X. L., Jiang, K. J., and Qiao, Z. G. (2013). Effect of salinity on the survival,growth and Na^+/K^+-ATPase activity of early juvenile mud crabs, Scylla paramamosain. *Mar. Sci.* 37 (2), 56–60.

Roberts, A., and Pachter, L. (2013). Streaming fragment assignment for real-time analysis of sequencing experiments. *Nat. Methods* 10 (1), 71–73. doi: 10.1038/nmeth.2251

Romano, N., and Zeng, C. S. (2012). Osmoregulation in decapod crustaceans: implications to aquaculture productivity, methods for potential improvement and interactions with elevated ammonia exposure. *Aquaculture* 334–337, 12–23. doi: 10.1016/j.aquaculture.2011.12.035

Roy, L. A., Davis, D. A., Saoud, I. P., Boyd, C. A., Pine, H. J., and Boyd, C. E. (2010). Shrimp culture in inland low salinity waters. *Rev. Aquac.* 2 (4), 191–208. doi: 10.1111/j.1753-5131.2010.01036.x

Shinji, J., Okutsu, T., Jayasankar, V., Jasmani, S., and Wilder, M. N. (2012). Metabolism of amino acids during hyposmotic adaptation in the whiteleg shrimp, litopenaeus vannamei. *Amino Acids* 43 (5), 1945–1954. doi: 10.1007/s00726-012-1266-2

Shi, X. Z., Zhao, X. F., and Wang, J. X. (2008). Molecular cloning and expression analysis of chymotrypsin-like serine protease from the Chinese shrimp, fenneropenaeus chinensis. *Fish Shellfish Immunol.* 25 (5), 589–597. doi: 10.1016/j.fsi.2008.07.011

Tadross, M. R., Dick, I. E., and Yue, D. T. (2008). Mechanism of local and global Ca^{2+} sensing by calmodulin in complex with a Ca^{2+} channel. *Cell* 133 (7), 1228–1240. doi: 10.1016/j.cell.2008.05.025

Tang, L., Wang, H., Wang, C. L., Mu, C. K., Wei, H. L., Yao, H. Z., et al (2020). Temperature potentially induced distinctive flavor of mud crab *Scylla paramamosain* mediated by gut microbiota. *Sci. Rep.* 10 (1), 3720. doi: 10.1038/s41598-020-60685-0

Wang, H., Tang, L., Wei, H. L., Lu, J. K., Mu, C. K., and Wang, C. L. (2018a). Transcriptomic analysis of adaptive mechanisms in response to sudden salinity drop in the mud crab, *Scylla paramamosain*. *BMC Genomics* 19 (1), 421. doi: 10.1186/s12864-018-4803-x

Wang, H., Wei, H. L., Tang, L., Lu, J. K., Mu, C. K., and Wang, C. L. (2018b). Identification and characterization of miRNAs in the gills of the mud crab (*Scylla paramamosain*) in response to a sudden drop in salinity. *BMC Genomics* 19 (1), 609. doi: 10.1186/s12864-018-4981-6

Wang, J., Zhang, P., Liu, N., Wang, Q., Luo, J., and Wang, L. (2015). Cadmium induces apoptosis in freshwater crab *Sinopotamon henanense* through activating calcium signal transduction pathway. *PloS One* 10 (12), e0144392. doi: 10.1371/journal.pone.0144392

Wu, Q. Y., Shi, C., Fang, S. B., Xie, Z. F., Guan, M. Y., Li, S. K., et al (2019). Different biochemical composition and nutritional value attribute to salinity and rearing period in male and female mud crab Scylla paramamosain. *Aquaculture* 513, 734417. doi: 10.1016/j.aquaculture.2019.734417

Xu, B. P., Tu, D. D., Yan, M. C., Shu, M. A., and Shao, Q. J. (2017). Molecular characterization of a cDNA encoding $Na^+/K^+/2Cl^-$ cotransporter in the gill of mud crab (*Scylla paramamosain*) during the molt cycle: Implication of its function in

osmoregulation. *Comp. Biochem. Physiol. A Mol. Integr. Physiol.* 203, 115–125. doi: 10.1016/j.cbpa.2016.08.019

Yao, H. Z., Li, X., Tang, L., Wang, H., Wang, C. L., Mu, C. K., et al (2020). Metabolic mechanism of the mud crab (*Scylla paramamosain*) adapting to salinity sudden drop based on GC-MS technology. *Aquac. Rep.* 18, 100533. doi: 10.1016/j.aqrep.2020.100533

Zhang, B. Q., and Wang, N. (2021). Study on the harm of saline alkali land and its improvement technology in China. *IOP Conf. Ser.: Earth Environ. Sci.* 692, 042053. doi: 10.1088/1755-1315/692/4/042053

Zhang, Y., Wu, Q. Y., Fang, S. B., Li, S. K., Zheng, H. P., Zhang, Y. L., et al (2020). mRNA profile provides novel insights into stress adaptation in mud crab megalopa, *Scylla paramamosain* after salinity stress. *BMC Genomics* 21 (1), 559. doi: 10.1186/s12864-020-06965-5

Zhao, Y., Wang, J., Thammaratsuntorn, J., Wu, J. W., Wei, J. H., Wang, Y., et al (2015). Comparative transcriptome analysis of Nile tilapia (*Oreochromis niloticus*) in response to alkalinity stress. *Genet. Mol. Res.* 14 (4), 17916–17926. doi: 10.4238/2015.December.22.16

Zhao, Y., Zhang, C. S., Zhou, H., Song, L. Y., Wang, J., and Zhao, J. L. (2020). Transcriptome changes for Nile tilapia (*Oreochromis niloticus*) in response to alkalinity stress. *Comp. Biochem. Physiol. Part D Genomics Proteomics* 33, 100651. doi: 10.1016/j.cbd.2019.100651

Zhou, M., Wang, A. L., and Xian, J. A. (2011). Variation of free amino acid and carbohydrate concentrations in white shrimp, *Litopenaeus vannamei*: Effects of continuous cold stress. *Aquaculture* 317 (1-4), 182–186. doi: 10.1016/j.aquaculture.2011.04.033